Nano Today xxx (xxxx) xxx

Contents lists available at ScienceDirect

Nano Today

journal homepage: www.elsevier.com/locate/nanotoday

Rapid Communication

Three dimension nanoparticle assemblies with tunable plasmonics via a layer-by-layer process

Thomas L. Derrien[a,b], Shogo Hamada[b], Max Zhou[b], Detlef-M. Smilgies[a,c,*], Dan Luo[b,*]

[a] Cornell High Energy Synchrotron Source (CHESS), Cornell University, Ithaca, NY 14853, United States
[b] Biological & Environmental Engineering, Cornell University, Ithaca, 14853, United States
[c] Chemical & Biomolecular Engineering, Cornell University, Ithaca, 14853, United States

ARTICLE INFO

Article history:
Received 29 September 2019
Accepted 9 December 2019
Available online xxx

Keywords:
Layer-by-layer
DNA nanotechnology
Plasmonics
Nanoparticle assembly

ABSTRACT

Recently, DNA has emerged as a designer material for the controlled assembly of nanoparticles. The unique programmability of Watson-crick base pairing offers limitless control over assembly via specific interactions. At the same time, reliance on non-specific interactions, such as layer-by-layer (LbL) assembly offers a simple assembly method, albeit with limited control. Here, by assembling DNA-capped gold nanoparticles in a LbL fashion we combine these two approaches and present a simple and robust method to construct large-scale three-dimensional nanoparticle assemblies with readily tunable plasmonics. Through variation of the DNA ligand and the nanoparticle core size the morphology of the three-dimensional nanoparticle assemblies was carefully adjustabed. These morphological changes, confirmed using grazing incidence x-ray scattering, enabled the tuning of the plasmonic behavior of the three-dimensional nanoparticle assemblies. The morphology could also be modified in real-time through water vapor induced swelling enabling dynamic tuning of the optical properties. The introduction of the DNA ligand to the LbL assembly method presented here imparted tunability to the process previously inaccessible with other nanoparticle ligands and presents a platform with which to create optically active materials of various compositions.

Introduction

One of the central goals of nanotechnology is to develop methods to control the arrangement of nanoscale building blocks in two and three dimensions, thus allowing researchers to control collective properties of nanoparticle. In plasmonics, of particular interest is the localized surface plasmon resonance (LSPR), whose frequency of can be modulated by coupling to neighboring nanoparticles. This coupling results in plasmon frequency shifts dictated by the arrangement of neighboring nanoparticles [1,2]. By controlling this arrangement, the plasmonics of nanoparticle assemblies can be precisely tuned to make designer metamaterials with unconventional optical properties [3–5].

One method to control the assembly of nanoparticles has been to employ an electrostatic fabrication technique in a process of layer-by-layer (LbL) assembly, whereby layers of oppositely charged nanoparticle and polyelectrolytes are alternately stacked to form three-dimensional (3D) assemblies. Such electrostatic assemblies were first shown for polyelectrolytes [6] and studies on nanoparticle-polyelectrolyte complexes soon followed [7–28]. This technique has enabled the construction of large-scale plasmonic assemblies of various nanoparticle compositions such as gold and silver, but precise control over the resultant morphology has been limited by the type of nanoparticle ligands employed and the nature of the polyelectrolyte layers [8,10,13,15].

This controllability problem can be addressed through the use of DNA as a nanoparticle ligand. DNA as a nanoscale organizer offers many advantages over conventional, non-DNA nanoparticle ligands such as alkylthiols and citrate. In this DNA-based approach, by conjugating short single-stranded DNA to the surface of nanoparticles, the programmability of the DNA afforded by Watson-Crick base-pairing can be imparted to the nanoparticles. The precise length and sequence control inherent to DNA have resulted a stunning variety of superlattice morphologies in one [29], two- [30–33], and three-dimensional [3,34–43] morphologies, including some whose lattice structures are not even found in nature [44,45]. While the unlimited combinatory nature of DNA base-pairing sequences affords limitless arrangement possibilities, reliance on base-pairing-mediated assembly is a double-edged sword: complex sequence design steps must be undertaken and the assembly must proceed

* Corresponding authors.
E-mail address: dl79@cornell.edu (D. Luo).

https://doi.org/10.1016/j.nantod.2019.100823
1748-0132/

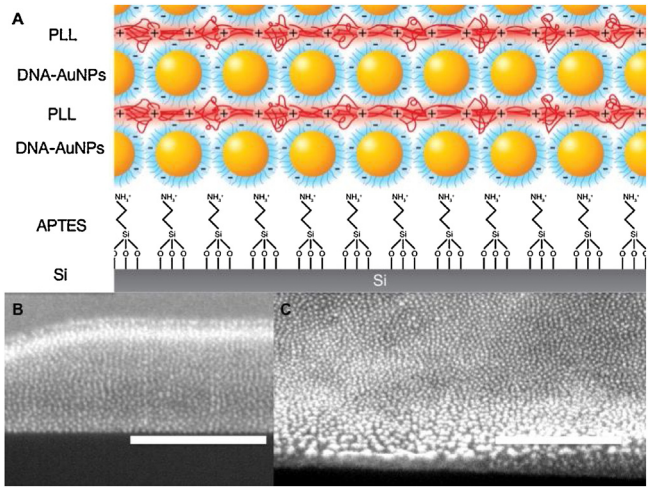

Fig. 1. Schematic representation of the 3Dnanoparticle assembly (A). FIB milled cross section with Pt overlayer (B) to avoid beam effects and without the Pt layer (C) enabling simultaneous scanning electron microscopy imaging of a cross section and the top layer of nanoparticles. Scale bar is 1 μm.

in a very narrow range of solution conditions (e.g., precise ionic strength, pH, etc). Additionally, DNA hybridization-based assembly limits the scalability of the nanoparticle constructs. Here, using a novel combination of non-base pairing DNA (single stranded DNA, ssDNA) and a LbL process, we construct large (centermeter) scale, 3D tunable plasmonic LbL nanoparticle assemblies.

The present strategy was inspired by our previous reports on the use of non-base pairing, ssDNA to construct nanoparticle assemblies. We have recently shown that single-stranded, non-base-pairing polythymine (PolyT) can be used to assemble two-dimensional (2D) nanoparticle superlattices at the air-water interface. Due to the negatively charged DNA backbone, the salt concentration in the nanoparticle solution determines the distance between particles;and this distance can be modified over a large range [30,33,46]. Our findings not only extended 2D nanoparticle crystallization to conditions relevant to real world applications, but also resulted in a semi-empirical and model to predict the behavior of the DNA organizer. Using these same assembly principles and our model at the air-water interface, we extended these phenomena to the liquid-solid interface to construct tunable plasmonic DNA-AuNP monolayers. Here, we added additional nanoparticle monolayers in a simple layer-by-layer (LbL) process in order to construct 3D nanoparticle assemblies with tunable plasmonics (Fig. 1A).

Materials and methods

Syntheses of DNA-capped gold nanoparticles (DNA-AuNPs)

Gold nanoparticles of various diameters (15, 20, and 30 nm were purchased from Ted Pella, inc. Oligonucleotides were purchased with a 5′ thiol modification from Integrated DNA Technologies. All solutions were prepared in 18.2 MΩ water. Oligonucleotides were de-protected using tris(2-carboethoxyethyl)-phosphine hydrochloride (TCEP- Sigma-Aldrich) in a 1:5 (DNA:TCEP) solution for 30 min. The thiol-terminal oligonucleotides were then added in excess (1:1200, 1:2100, 1:4725, AuNP:DNA ratio for the 15, 20, and 30 nm AuNPs, respectively) to a solution of AuNPs and then shaken overnight at 500 rom. NaCl was then slowly added in 50 mM increments over a period of 8 h to final concentration of 500 mM. Purification was then undertaken via several centrifugation cycles in pure water. Polythymine oligonucleotides were chosen to maximize stability against the high $MgCl_2$ concentrations used in the preparation of the nanoparticle assemblies{mirkin}.

Preparation of LbL nanoparticle assemblies

Three-dimensional nanoparticle assemblies were prepared on 3-aminopropyl triethoxysilane (APTES, Sigma-Aldrich) functionalized glass substrates. Silanization was performed by incubating the piranha cleaned glass microscope slide substrate in a 2 % APTES solution in 95 % ethanol overnight. The substrates were then rinsed in ethanol and isopropanol followed by baking at 95 °C for 1 h before a final rinsing cycle. The freshly silanized glass substrates were then used to attach an initial layer of DNA-AuNPs by incubating an aqueous solution of DNA-AuNPs (∼10 nM DNA-AuNPs, 250 mM ionic strength MgCl2) overnight. After thorough rinsing in water to removed the unattached DNA-AuNPs a 1 mg/mL poly-l¬-lysine hydrobromide (PLL, 300 kD, Sigma-Aldrich) solution was incubated on the DNA-AuNP monolayer for 30 min. The process was repeated to reach the desired number of DNA-AuNP layers.

Large-scale plasmonic assemblies were prepared on a APTES functionalized microscope slide. A silicone stencil was pressed onto the slide and solutions of DNA-capped gold nanoparticle and PLL were alternated until the desired layer number was achieved.

Absorbance and reflectance measurements

Optical spectra were obtained with a Filmetrics F40 instrument. Reflectance spectra were taken with the instrument's built-in light source, while absorbance spectra were taken using an external halogen light source that could be coupled to GISAXS chamber.

Grazing incidence small-angle X-ray scattering (GISAXS) experiments

GISAXS experiments were performed on the dried multilayer nanoparticle samples at the D1 experimental station at the Cornell High Energy Synchrotron Source (CHESS). D1 uses a multilayer monochromator to deliver an incident x-ray beam with a flux of ∼1012 photons s-1 mm-1 with a 1.5 % bandwidth and 1.16 Å wavelength. A Pilatus 200 K detector, with a pixel size of 172 × 172 μm with a sample-to-detector distance of 1835 mm was used. The incident x-ray beam angle was 0.25°. Solvent vapor annealing using water vapor was performed in a specialized chamber described elsewhere (source).

Results and discussion

Plasmonic LbL assemblies were constructed by first functionalizing a cleaned glass substrate with (3-amino)propyltriethoxysilane (APTES). The APTES imparted a positive charge to the glass surface to facilitate the adsorption of the negatively charged DNA-AuNPs. AuNP monolayers were then deposited by incubating a DNA-AuNP droplet in 250 mM ionic strength (IS) $MgCl_2$ to ensure densely packed assemblies. After rinsing unbound DNA-AuNPs with water, poly-L-lysine hydrobromide (PLL) (300 kDa) was attached on top of the DNA-AuNP monolayer. The newly laid, positively charged PLL layer enabled an additional DNA-AuNP monolayer to be deposited and the process was repeated until the desired number of layers was achieved (Fig. 1A). In our case we used a biocompatible and a readily tunable DNA nanoparticle ligand. The use of the DNA ligand afforded a distinct advantage over smaller organic [8–12] and hydrophilic [13–28] ligands previously used, whose tunability is greatly limited by their size. The length of the DNA ligand, on the other hand, could be varied from ∼6–15 nm, by simply changing the number of thymine bases.

Please cite this article as: T.L. Derrien, S. Hamada, M. Zhou et al., Three dimension nanoparticle assemblies with tunable plasmonics via a layer-by-layer process, Nano Today, https://doi.org/10.1016/j.nantod.2019.100823

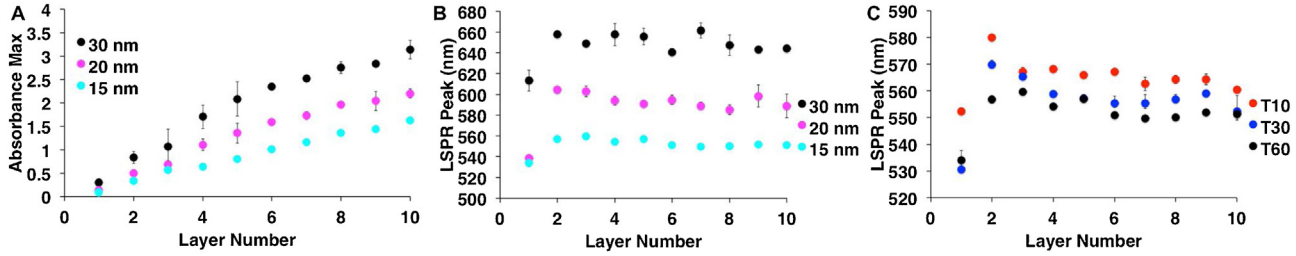

Fig. 2. Optical characterization of the LbL nanoparticle superstructures. The absorbance maxima of the assemblies could be tuned by varying the number of nanoparticle layers as well as the nanoparticle core size (A). The plasmonics of these assemblies could also be selectively tuned through changing the core size (B) and the DNA ligand length (C) as seen by the position of the LSPR peaks.

Gold nanoparticles are well-known for their strong plasmonic response [47,48]. Several plasmonic assemblies were constructed via this method by varying the DNA ligand length and the nanoparticle core size. Three DNA ligand lengths [polythymine oligonucleotides of 10 (T10), 30 (T30), and 60 (T60) bases] and three nanoparticle core sizes (15, 20, and 30 nm) were used; each system displayed unique properties. To study the morphology of the deposited multilayers, scanning electron microscopy (SEM) was undertaken after focused ion beam (FIB) milling. The FIB milling was performed after depositing a Pt layer, in order to avoid edge defects so as to obtain a clean cross-section (Fig. 1B). Here the nanoparticle stacking is clearly seen, although no long-range order is apparent while local order is visible. FIB milling was also performed without the Pt layer, enabling SEM imaging of the top layer of nanoparticles (Fig. 1C), albeit with visible ion beam effects. In this case local hexagonal packing is seen, though again, without evidence of long-range order.

A unique advantage of the LbL approach to building plasmonic nanoparticle multilayers is that it allows precise control over the amount of nanomaterial deposited. In our system, this enabled the tunability of the optical properties of the 3D nanoparticle assemblies. Specifically, we tuned the reflectivity, the absorbance magnitude, and the localized surface plasmon resonance peak wavelength by varying the number of nanoparticle layers deposited. Sample absorbance traces are shown for the first five layers of 15 nm core nanoparticle with a T60 ssDNA ligand in Figure S2. A key feature of the LbL method is that roughly the same amount of nanoparticles was contained within each layer, as illustrated by the linear increase in the absorbance maximum (Fig. 2A, S22). This was the case for all the nanoparticle core sizes tested (15, 20, and 30 nm), which highlighted the robustness and reproducibility of our method. While the absorbance increased linearly, the LSPR maximum typically reached a maximum wavelength after the addition of two to three nanoparticle layers (Fig. 2B, C). Upon addition of the first layers, the LSPR underwent the characteristic red-shift typically observed in nanoparticle assemblies due to coupled LSPRs [49]. However, on addition of the next layer, a distinctive blue-shift was seen before stabilizing to a final LSPR wavelength following the addition of subsequent nanoparticle layers. Fig. 2 highlights the influence of the nanoparticle size on both the absorbance (Fig. 2A), as expected due to the increased scattering cross section, and the plasmonics (Fig. 2B), as can be calculated from the universal plasmon ruler proposed by Jain and El-Sayed [49]. In addition to the ability to tune the absorbance, the LbL assembly provided a platform through which to control the reflectance of the assembled nanoparticle films. The reflectance reached a maximum value with the addition of a fourth nanoparticle layer, after which it began to decrease (Figure S4). The use of the ssDNA capping ligand afforded an additional tunable parameter, i.e., the DNA length. Three distinct ssDNA lengths of 10, 30, and 60 thymine bases (T10, T30, and T60, respectively) were used with 15 nm nanoparticle core sizes. Similar to the data in Fig. 2, the optical properties of absorbance

Fig. 3. Construction of large-scale plasmonic nanoparticle assemblies demonstrating the tunability of the absorbance (top) and reflectance (bottom).

maximum (Figure S3) and LSPR wavelength (Fig. 2B) of the assemblies were tuned by varying the ssDNA length. As well as allowing flexibility through the use of the variable ligand, DNA, the combination with LBL assembly imparts optical tunability inaccessible with monolayer systems which is advantageous in opetoelectronic devices where wavelength specificity is needed.

The LbL process provides at least three tunable parameters to build 3D nanoparticle superstructures: 1) nanoparticle core size, 2) ssDNA ligand length, and 3) nanoparticle layer number. Combined with the aforementioned optical characterizations, this LbL process offers the potential to create materials with a wide range of optical properties. To illustrate the tunable plasmonics of the system, we created a stencil to highlight the variations by adjusting the nanoparticle core size and layer number. Each letter in the stenciled pattern contained an LbL assembly with a unique composition, of either 15, 20, or 30 nm nanoparticle core size and up to 4 nanoparticle layers (each with T60 DNA ligands), thereby exhibiting distinct optical properties (Fig. 3). Note that the resulting photograph was taken on a transilluminator with the light source switched on (top) or off (bottom) so as to demonstrate the changes in absorbance and reflectivity of the system. Our data not only depicted the diversity of the properties available with this simple system but the large scale at which these assemblies were produced. Each letter was approximately 10 mm in width, and the total pattern covers approximately 570 mm^2, thus highlighting the scalability of our LbL process. Moreover, these bulk-scale 3D nanoparticle superstructures remained stable in a variety of solutions (acetone, ethanol, and up to 500 mM ionic strength $MgCl_2$, data not shown), potentially facilitating their use for optoelectronic devices needing to operate in harsh environments.

The tunable plasmonics indicated that the morphology of the 3D nanoparticle superstructures varied considerably upon changing the nanoparticle core size and the DNA ligand length. In order to probe this variation, we employed grazing incidence small angle x-ray scattering (GISAXS) to study films consisting of 10 nanoparticle layers. The integrated spectra (Fig. 4), like the SEM images, indicated no long-range order, as shown by the presence of a single broad first-order Bragg peak. However, important information regarding the average morphology of the various 3D nanoparticle

Please cite this article as: T.L. Derrien, S. Hamada, M. Zhou et al., Three dimension nanoparticle assemblies with tunable plasmonics via a layer-by-layer process, Nano Today, https://doi.org/10.1016/j.nantod.2019.100823

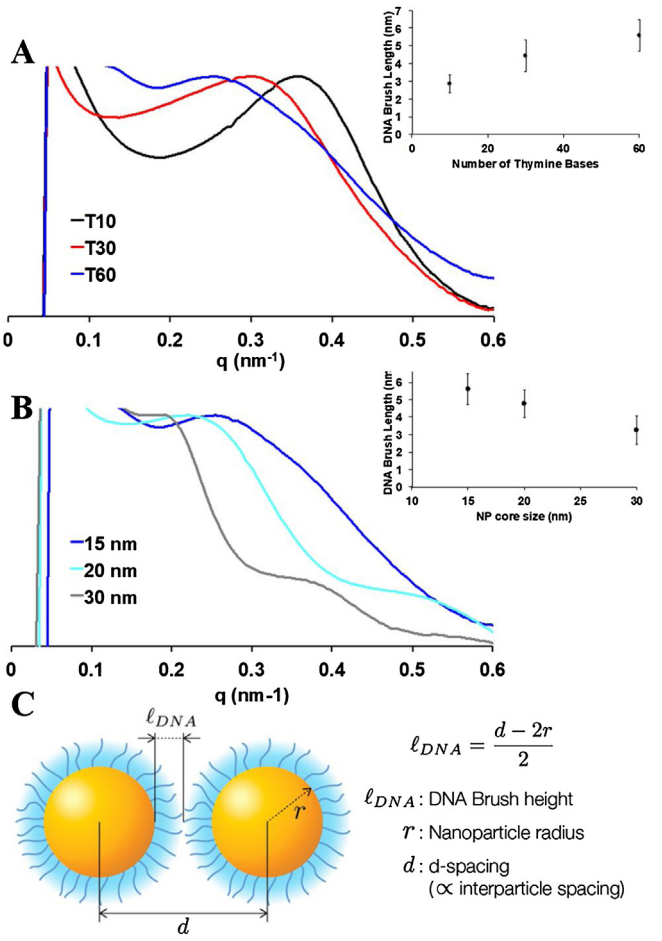

Fig. 4. Small angle x-ray scattering morphological characterization of the 3D nanoparticle assemblies for samples prepared with 15 nm AuNPs and several ligand lengths (A) and with T60 DNA ligands and several AuNP core sizes (B). The peak shift to higher q values indicated the shrinking of the d- spacings by shortening the ligand length, or through use of larger nanoparticle cores, as also confirmed in the insets indicating the of the length of the DNA ligand brush in the samples. GISAXS spectra were normalized to the same magnitude to facilitate comparison of the peak positions. (C) Calculation of the DNA brush length.

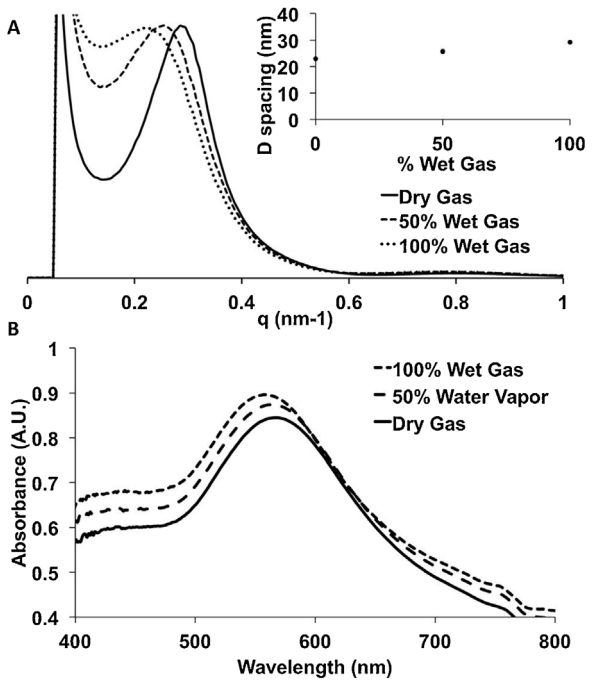

Fig. 5. Solvent vapor annealing of a 5-layer 3D nanoparticle assembly. The sample was swelled by introduction of water vapor into the sample chamber, which was used to tune the morphology and optical properties of the sample. GISAXS spectra show the change in nanoparticle spacings, as indicated by the shift of the firs-order peaks to lower q-values with increasing water vapor amounts (A). The inset displays the calculated nanoparticle spacings obtained for the varying amounts of water vapor. The shift in the nanoparticle spacings was accompanied by a shift in the absorbance of the nanoparticles (B). GISAXS spectra were normalized to the same magnitude to facilitate comparison of the peak positions.

superstructures can be gleaned. Notably, the d-spacing, where $d = 2\pi/q$ (q is the position of first-order Bragg peak), within the 3D nanoparticle assemblies was enlarged by increasing the 1) number of thymine bases on the DNA ligand, and 2) nanoparticle core size. In samples composed of 3D assemblies with 15 nm gold nanoparticles, this was seen by the shift of the first-order Bragg peak to lower q values upon the use of longer DNA ligands, indicating a larger d-spacing (Fig. 4A). Similarly, in samples employing T60 ligands with various nanoparticle core sizes, the peak positions of the first-order peak indicated a larger d-spacing for larger nanoparticles (Fig. 4B). From the measured d-spacings, an approximate DNA brush length was estimated by subtracting the contribution of the nanoparticle cores (insets Fig. 4C). It should be noted that without a crystallographic arrangement (i.e. long-range order), the exact nearest-neighbor spacing of the nanoparticles, and therefore the DNA brush length, could not be calculated. However, the approximations employed herein provided an important insight into the trends of the DNA ligand shell. For example, we found that larger nanoparticle cores resulted in shorter DNA brush lengths (inset Fig. 4B) than smaller nanoparticle cores, indicating the stronger interparticle attraction between particles of larger size [50]

The number of variable parameters characterized above established a platform through which to tune the morphology of the 3D nanoparticle assemblies. Additional tunability could be imparted in real-time to create a dynamic system through swelling of the samples in humid environments. This was achieved through the use of a specialized solvent vapor annealing (SVA) chamber which allowed *in-situ* monitoring of the optical and GISAXS spectra while simultaneously enabling the precise control of solvent vapors over the sample (SI). A sample composed of 5 layers of 15 nm gold nanoparticles with T60 ligands was swelled by changing the composition of gas over the sample from dry gas (dry N_2) to 100 % wet gas (N_2 bubbled through water). The change from dry to wet gas was accompanied by a marked shift of the first-order peak to lower q values, indicating an increase of the nanoparticle d spacing (Fig. 5A), as well as of the DNA brush length (Fig. 5A, inset). Because of the swelling of the nanoparticle assemblies, the wavelength of the LSPR was blue-shifted by approximately 9 nm (Fig. 5B). Interestingly, the d-spacings and the LSPR positions in dry gas were slightly smaller than those previously measured in ambient conditions, presumably due to the drying effect of the N_2 gas and the residual ambient humidity.

Conclusions

The strict layer-by-layer process described here, with alternating layers of DNA-capped gold nanoparticles and PLL polyelectrolyte, provided a platform through which to produce large-scale 3D nanoparticle superstructures with readily tunable plasmonics. The morphology of the nanoparticle assemblies, and therefore the plasmonic behavior, was precisely controlled through variation of the DNA ligand length and the nanoparticle core size; this level of control has been very difficult to obtain with the use of smaller ligands. The resultant morphological alterations, confirmed via GISAXS studies, enabled the construction of bulk-scale assemblies with widely variable plasmonic properties. Finally, through

Please cite this article as: T.L. Derrien, S. Hamada, M. Zhou et al., Three dimension nanoparticle assemblies with tunable plasmonics via a layer-by-layer process, Nano Today, https://doi.org/10.1016/j.nantod.2019.100823

water vapor induced swelling of the nanoparticle assemblies in real-time, the morphology and optical properties could also be dynamically tuned. This robust strategy to produce 3D nanoparticle assemblies could be readily adapted to other nanoparticles that can be functionalized with DNA, such as quantum dots [51–54], silver [3,55–57], and upconverting nanoparticles [58,59], in order to produce bulk-scale optically active materials over a broad spectral range.

Funding sources

No competing financial interests have been declared.

Acknowledgments

T.L.D. acknowledges support from NSF IGERT under DGE-0903653. This research is funded by NSF award SNM-1530522 and is based upon work at the Cornell High Energy Synchrotron Source (CHESS) which is supported by the NSF & NIH/NIGMH via NSF award DMR-1332208. This work also made use of the Cornell Center for Materials Research (CCMR) shared facilities supported by DMR-1719875.

Appendix A. Supplementary data

Supplementary material related to this article can be found, in the online version, at doi:https://doi.org/10.1016/j.nantod.2019.100823.

References

[1] R. Yu, L.M. Liz-Marzan, F.J. Garcia de Abajo, Chem. Soc. Rev. 46 (2017) 6710–6724.
[2] S.J. Tan, M.J. Campolongo, D. Luo, W. Cheng, Nat. Nanotechnol. 6 (2011) 268–276.
[3] K.L. Young, M.B. Ross, M.G. Blaber, M. Rycenga, M.R. Jones, C. Zhang, A.J. Senesi, B. Lee, G.C. Schatz, C.A. Mirkin, Adv Mater 26 (2014) 653–659.
[4] J. Henzie, M.H. Lee, T.W. Odom, Nat. Nanotechnol. 2 (2007) 549–554.
[5] D.B. Litt, M.R. Jones, M. Hentschel, Y. Wang, S. Yang, H.D. Ha, X. Zhang, A.P. Alivisatos, Nano Lett. 18 (2018) 859–864.
[6] G. Decher, Science 277 (1997) 1232.
[7] J. Lee, P. Hernandez, J. Lee, A.O. Govorov, N.A. Kotov, Nat. Mater. 6 (2007) 291–295.
[8] E.W. Chan, D.C. Lee, M.K. Ng, G. Wu, K.Y. Lee, L. Yu, J. Am. Chem. Soc. 124 (2002) 12238–12243.
[9] F.P. Zamborini, L.E. Smart, M.C. Leopold, R.W. Murray, Anal. Chim. Acta 496 (2003) 3–16.
[10] H.L. Zhang, S.D. Evans, J.R. Henderson, Adv. Mater. 15 (2003) 531–534.
[11] X. Zhou, C. Liu, Z. Zhang, L. Jiang, J. Li, J. Colloid Interface Sci. 284 (2005) 354–357.
[12] S.Y. Heriot, H.-L. Zhang, S.D. Evans, T.H. Richardson, Colloids Surf. A Physicochem. Eng. Asp. 278 (2006) 98–105.
[13] J.F. Hicks, Y. Seok-Shon, R.W. Murray, Langmuir 18 (2002) 2288–2294.
[14] N. Krasteva, I. Besnard, B. Guse, R.E. Bauer, K. Müllen, A. Yasuda, T. Vossmeyer, Nano Lett. 2 (2002) 551–555.
[15] Y. Fu, H. Xu, S. Bai, D. Qiu, J. Sun, Z. Wang, X. Zhang, Macromol. Rapid Commun. 23 (2002) 256–259.
[16] H. Huang, X. Yang, Colloids Surf. A Physicochem. Eng. Asp. 226 (2003) 77–86.
[17] W. Song, M. Okamura, T. Kondo, K. Uosaki, J. Electroanal. Chem. 554-555 (2003) 385–393.
[18] S. Ghannoum, Y. Xin, J. Jaber, L.I. Halaoui, Langmuir 19 (2003) 4804–4811.
[19] N. Ferreyra, L. Coche-Guerente, J. Fatisson, M. Lopez Teijelo, P. Labbe, Chem. Commun. (Camb.) (2003) 2056–2057.
[20] P.J. Kulesza, M. Chojak, K. Karnicka, K. Miecznikowski, B. Palys, A. Lewera, A. Wieckowski, Chem. Mater. 16 (2004) 4128–4134.
[21] M. Carrara, J.J. Kakkassery, J.P. Abid, D.J. Fermin, ChemPhysChem 5 (2004) 571–575.
[22] Z. Qi, I. Honma, M. Ichihara, H. Zhou, Adv. Funct. Mater. 16 (2005) 377–386.
[23] H.A. Santos, M. Chirea, V. Garcia-Morales, F. Silva, J.A. Manzanares, K. Kontturi, J. Phys. Chem. B 109 (2005) 20105–20114.
[24] M. Chirea, V. Garcia-Morales, J.A. Manzanares, C. Pereira, R. Gulaboski, F. Silva, J. Phys. Chem. B 109 (2005) 21808–21817.
[25] C.M.P. Mariana Chirea, Fernando Silva, J. Phys. Chem. C 111 (2007) 9255–9266.
[26] A.A. Galyean, R.W. Day, J. Malinowski, K.W. Kittredge, M.C. Leopold, J. Colloid Interface Sci. 331 (2009) 532–542.
[27] A. Liu, G. Abbineni, C. Mao, Adv. Mater. 21 (2008) 1001–1005.
[28] N. Higashi, T. Takagi, T. Koga, Polym. J. 42 (2010) 95.
[29] Y.P. Ohayon, R. Sha, O. Flint, W. Liu, B. Chakraborty, H.K.K. Subramanian, J. Zheng, A.R. Chandrasekaran, H.O. Abdallah, X. Wang, X. Zhang, N.C. Seeman, ACS Nano 9 (2015) 10304–10312.
[30] S.J. Tan, J.S. Kahn, T.L. Derrien, M.J. Campolongo, M. Zhao, D.M. Smilgies, D. Luo, Angew. Chem. Int. Ed. Engl. 53 (2014) 1316–1319.
[31] W. Cheng, M.J. Campolongo, J.J. Cha, S.J. Tan, C.C. Umbach, D.A. Muller, D. Luo, Nat. Mater. 8 (2009) 519–525.
[32] W.L. Cheng, N.Y. Park, M.T. Walter, M.R. Hartman, D. Luo, Nat. Nanotechnol. 3 (2008) 682–690.
[33] T.L. Derrien, M. Zhang, P.O. Dorion, D.M. Smilgies, D. Luo, Langmuir (2018).
[34] H.D. Hill, R.J. Macfarlane, A.J. Senesi, B. Lee, S.Y. Park, C.A. Mirkin, Nano Lett. 8 (2008) 2341–2344.
[35] M.R. Jones, R.J. Macfarlane, B. Lee, J. Zhang, K.L. Young, A.J. Senesi, C.A. Mirkin, Nat. Mater. 9 (2010) 913–917.
[36] R.J. Macfarlane, M.R. Jones, B. Lee, E. Auyeung, C.A. Mirkin, Science 341 (2013) 1222–1225.
[37] R.J. Macfarlane, B. Lee, M.R. Jones, N. Harris, G.C. Schatz, C.A. Mirkin, Science 334 (2011) 204–208.
[38] S.Y. Park, A.K. Lytton-Jean, B. Lee, S. Weigand, G.C. Schatz, C.A. Mirkin, Nature 451 (2008) 553–556.
[39] F. Lu, K.G. Yager, Y. Zhang, H. Xin, O. Gang, Nat. Commun. 6 (2015) 6912.
[40] M.M. Maye, M.T. Kumara, D. Nykypanchuk, W.B. Sherman, O. Gang, Nat. Nanotechnol. 5 (2010) 116–120.
[41] D. Nykypanchuk, M.M. Maye, D. van der Lelie, O. Gang, Nature 451 (2008) 549–552.
[42] S. Pal, Y. Zhang, S.K. Kumar, O. Gang, J. Am. Chem. Soc. 137 (2015) 4030–4033.
[43] Y. Zhang, S. Pal, B. Srinivasan, T. Vo, S. Kumar, O. Gang, Nat. Mater. 14 (2015) 840–847.
[44] E. Auyeung, J.I. Cutler, R.J. Macfarlane, M.R. Jones, J. Wu, G. Liu, K. Zhang, K.D. Osberg, C.A. Mirkin, Nat. Nanotechnol. 7 (2011) 24–28.
[45] W. Liu, M. Tagawa, H.L. Xin, T. Wang, H. Emamy, H. Li, K.G. Yager, F.W. Starr, A.V. Tkachenko, O. Gang, Science 351 (2016) 582–586.
[46] M.J. Campolongo, S.J. Tan, D.M. Smilgies, M. Zhao, Y. Chen, I. Xhangolli, W. Cheng, D. Luo, ACS Nano 5 (2011) 7978–7985.
[47] S. Link, M.A. El-Sayed, Annu. Rev. Phys. Chem. 54 (2003) 331–366.
[48] C.C. DuFort, B. Dragnea, Annu. Rev. Phys. Chem. 61 (2010) 323–344.
[49] P.K. Jain, M.A. El-Sayed, Nano Lett. 7 (2007) 2854–2858.
[50] H.C. Hamaker, Physica 4 (1937) 1058–1072.
[51] G.P. Mitchell, C.A. Mirkin, R.L. Letsinger, J. Am. Chem. Soc. 121 (1999) 8122–8123.
[52] D. Huang, C. Niu, X. Wang, X. Lv, G. Zeng, Anal. Chem. 85 (2013) 1164–1170.
[53] Z. Deng, A. Samanta, J. Nangreave, H. Yan, Y. Liu, J. Am. Chem. Soc. 134 (2012) 17424–17427.
[54] D. Sun, O. Gang, J. Am. Chem. Soc. 133 (2011) 5252–5254.
[55] Cao, R. Jin, C.A. Mirkin, J. Am. Chem. Soc. 123 (2001) 7961–7962.
[56] J.-S. Lee, A.K.R. Lytton-Jean, S.J. Hurst, C.A. Mirkin, Nano Lett. 7 (2007) 2112–2115.
[57] S. Pal, J. Sharma, H. Yan, Y. Liu, Chem. Commun. (2009) 6059–6061.
[58] L.-J. Huang, R.-Q. Yu, X. Chu, Analyst 140 (2015) 4987–4990.
[59] D. Mendez-Gonzalez, M. Laurenti, A. Latorre, A. Somoza, A. Vazquez, A.I. Negredo, E. López-Cabarcos, O.G. Calderón, S. Melle, J. Rubio-Retama, ACS Appl. Mater. Interfaces 9 (2017) 12272–12281.

Thomas L. Derrien is a post-doctoral research associate at the Diamond Light Source in Didcot, United Kingdom. He received a B.Sc. and a M.Sc. from McGill University, Canada before completing his Ph.D. in 2017 at Cornell University, USA. During his Ph.D. he studied nanoparticle self-assembly making copious use of the Cornell High Energy Synchrotron (CHESS). After his Ph.D. he completed a brief post-doc at CHESS before moving to his present position at Diamond Light Source where he works on materials characterization using synchrotron X-ray scattering.

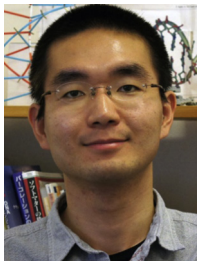

Shogo Hamada is a Research Associate of Luo lab and a Lecturer in the Department of Biological and Environmental Engineering at Cornell University. After working as an Assistant Professor in the Department of Bioengineering and Robotics at Tohoku University (Japan), he became a Kavli Postdoctoral Fellow in the Kavli Institute at Cornell for Nanoscale Science at Cornell University. His research interest lies at the intersection between nano-bioengineering and robotics, including DNA-based dynamic assemblies.

Please cite this article as: T.L. Derrien, S. Hamada, M. Zhou et al., Three dimension nanoparticle assemblies with tunable plasmonics via a layer-by-layer process, Nano Today, https://doi.org/10.1016/j.nantod.2019.100823

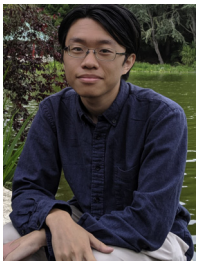

Max received a B.S. in Biological Engineering and in Computer Science from Cornell University in 2019. His current research interests are in computational biology and machine learning. Currently, he is working as a software engineer outside of academia.

Detlef-M. Smilgies is a retired beamline scientist and has worked in synchrotron radiation science for over 25 years. His interest is in grazing-incidence scattering methods for the study of interfaces and thin films of soft materials. These include nanoparticles superlattices, materials for organic electronics, and block copolymer nanostructures. His research focus has been the development of real-time in-situ characterization of self-assembly processes. He currently is an adjunct professor of chemical and biomolecular engineering at Cornell University and a visiting scientist at Binghamton University.

Dan Luo obtained his BS from University of Science and Technology of China in 1989 and PhD in 1997 from The Ohio State University. After his postdoctoral training in the School of Chemical Engineering at Cornell University, he joined Cornell faculty in the Department of Biological and Environmental Engineering as an assistant professor in 2001 and was promoted to full professor in 2011. His research interest focuses on engineering DNA as both a generic and a genetic material for real-world applications.

Please cite this article as: T.L. Derrien, S. Hamada, M. Zhou et al., Three dimension nanoparticle assemblies with tunable plasmonics via a layer-by-layer process, Nano Today, https://doi.org/10.1016/j.nantod.2019.100823